

Model-Prototype Correlation of Mixing
in a Wastewater Dechlorination Basin

H. G. Stefan,¹ T. R. Johnson,² H. McConnell,³ and C. Anderson⁴

Purpose of Study

The turbulent mixing characteristics of a municipal wastewater dechlorination basin (Fig. 1) were studied in a 1:12 scale sectional model and in the field using conservative tracers. Comparison and interpretation of this data is the objective of this paper.

The purpose of dechlorination is to chemically remove residual chlorine after disinfection because it is toxic and harmful to organisms in the receiving water. A dechlorination basin is a reactor basin in which a solution of SO_2 in water is injected into the chlorinated effluent of a wastewater treatment plant. The SO_2 reacts with the residual chlorine. For the reaction to be complete, the injected SO_2 must become thoroughly mixed with the residual chlorine. In the case study presented, this did originally not occur. Subsequently, modifications were made in the basin to increase mixing. The model study was conducted to determine the effectiveness of different basin modifications.

Flow Geometry

The dechlorination basin studied is at the Metropolitan Wastewater Treatment Plant, St. Paul, Minnesota, and is shown in Fig. 1. It is located at the end of a 250 m long trapezoidal chlorine contact channel. The wastewater enters the basin through six 1.4 m x 2.6 m ports in a baffle wall and leaves over nine 2.6 m wide weirs to be discharged into a side channel of the Mississippi River. A vertical section and a plan view of the center portion of the 1:12 scale basin model are shown in Fig. 2. The column wall was an addition to the original design. The flow rate can vary from 0.27 to 1.01 m^3s^{-1} per meter basin width with a mean daily design flow of 0.39 m^3s^{-1} . The weir at the end of the dechlorination basin, controls the water level in the dechlorination basin at normal river stage.

The SO_2 solution is injected into the chlorinated water upstream of the baffle wall ports at a rate of 0.016 m^3/s . The original injection system consisted of a 14.6 m long, horizontal diffuser with one row of 8 mm diameter holes through which SO_2 was injected in a horizontal upstream direction. To induce mixing and aeration, air was injected downstream from the baffle wall at a rate of 21.2 m^3/min through a horizontal diffuser of 14.6 m length.

¹Professor and Associate Director, ²Research Assistant, St. Anthony Falls Hydraulic Laboratory, Department of Civil & Mineral Engineering, University of Minnesota, Minneapolis, MN 55414.

³Project Leader, ⁴Research Engineer, Metropolitan Waste Control Commission, St. Paul, MN 55101.

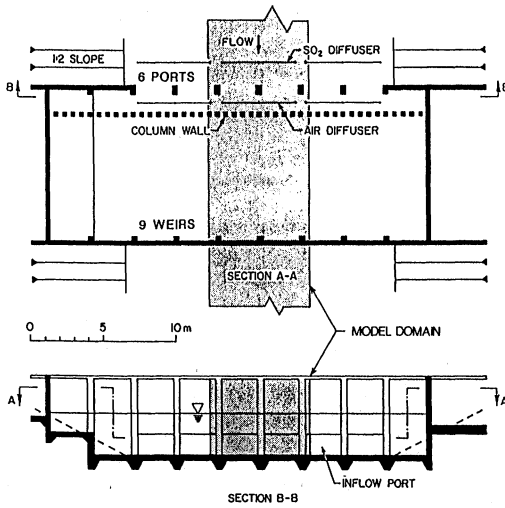


Fig. 1. Dechlorination basin geometry, prototype.

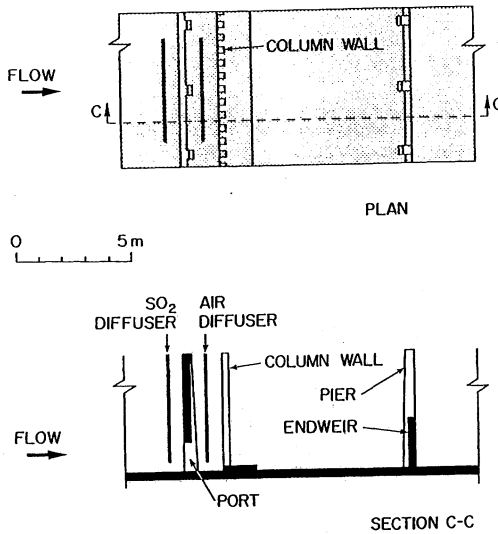


Fig. 2. Dechlorination basin model. Final design. Dimensions are for full scale.

Similarity Criteria

Flow and turbulent mixing in the dechlorination basin had to be modeled. For this purpose, full Reynolds similarity would be desirable. The flow over the weir at the end of the basin is a gravity flow requiring Froude scaling. The overall flow field is driven by gravity. Therefore, the model was designed and built as a free surface flow section using Froude similarity. The model was a "sectional model" of only the center portion of the basin, mostly to reduce cost. The scale was kept large (1:12) so that Reynolds numbers based on inlet port depth would remain above 10,000 in the model. Even so, the Reynolds numbers in the prototype were 40 times larger.

Inspection of the flow field in the model (Fig. 3) revealed several flow features which can depend on Reynolds number: the contraction to the inlet port, the wall-jet-like underflow through the port, the large recirculation region behind the baffle wall. If the model Reynolds number of 10,000 is not far enough into the turbulent range, differences in the model-prototype flow fields and mixing may appear.

An additional scaling problem was created by the air injected behind the inlet wall (Fig. 3). The air flow rate was scaled using Froude similarity so that the initial buoyancy effects are similar. The bubble size and rise velocities could be scaled exactly because orifice size could not be scaled 1:12. In the model bubbles appeared on the water surface closer to the inlet wall than in the prototype.

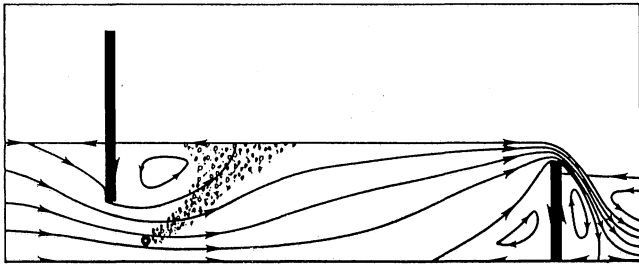


Fig. 3. Streamline pattern in original dechlorination basin design.
Flow = $0.27 \text{ m}^3/\text{s}$ per meter width.

Data Collected

Concentration time series of dye or salt injected through the SO_2 diffuser were collected in both the model and field to assess mixing. Conservative tracers were used to represent the reactive chemicals. Statistical parameters such as mean, standard deviation, and skewness of the signal distributions were calculated. Spectra were also extracted from the time series, using a fast Fourier transform program written by Stanley and Peterson (1973). Definitions are given in the appendix.

Results

Case I - Original Conditions - The original basin geometry was a shown in Fig. 1 but without the column wall and with the SO_2 injection at a single elevation. The original design exhibited incomplete mixing of the chemicals within the basin. (McConnell, 1986).

In the field Rhodamine WT was injected for 7 minutes through the sulfur dioxide solution injection system and the dye concentration was measured at 15 points on the basin centerline (Fig. 4). The effluent sample was withdrawn continuously with a submersible pump, and the concentration measured with a Turner Model III Fluorometer equipped with a flowthrough cell. The concentration was recorded on a chart recorder as a continuous trace.

In the model, a salt solution was injected into the SO_2 injection system for 2 minutes (equivalent of 7 minutes). Conductivity was measured at the same 15 points along the basin centerline with a conductivity meter. Distance between the electrodes was 0.5 cm. The output was recorded on a chart recorder as a continuous trace.

Both the model and field time series were digitized using a Houston Instrument III-PAD Digitizer connected to an Apple II computer. The peaks and valleys and some intermediate points were recorded at first, then discretized values at regular intervals (1 sec) were determined by linear interpolation between the digitized data points. Some of the extreme values were lost in the second process.

The determination of statistical parameters required the extraction of the steady-state portion of the time series. The values were also adjusted for baseline drift by assuming a constant baseline slope.

Figure 4 shows the mean concentrations measured at each of the 15 points in both the model and prototype.

Standard error between all model and prototype mean concentrations was 0.55. The standard error of the mean concentrations in the basin was 0.39. The standard error of the mean concentrations measured at the six most downstream data points was 0.25. Isoleths are drawn from each set of measurements. The general shape of the dye plume inside the dechlorination basin before the structural modification is similar for both the sectional model and the prototype tests. The greater width of the plume in the prototype probably indicates greater turbulent spreading in the prototype than in the model. The concentration fluctuations, characterized by the standard deviations and skewness (Figs. 5 and 6), are larger in the model than in the prototype, also indicating a relatively less well mixed system in the model. This is probably related to the differences in turbulence indicated by the Reynolds numbers in the model and prototype as discussed later.

The tracer plume also appears to rise somewhat faster in the prototype basin than in the model basin. There is a separated flow region extending from the bottom of the overflow weir upstream into the basin (Fig. 3). In the model, that region is relatively small (Fig. 3). In the prototype, it can be inferred from the isopleths and appears larger. It is shown as a dotted line in Fig. 4.

The spectral analysis shows more high frequency, small-scale fluctuations in the model than in the field. Figure 7 has examples. (In Fig. 7, the frequency scales are the same for model and prototype, whereas the amplitudes are not scaled.)

MODEL PROTOTYPE CORRELATION

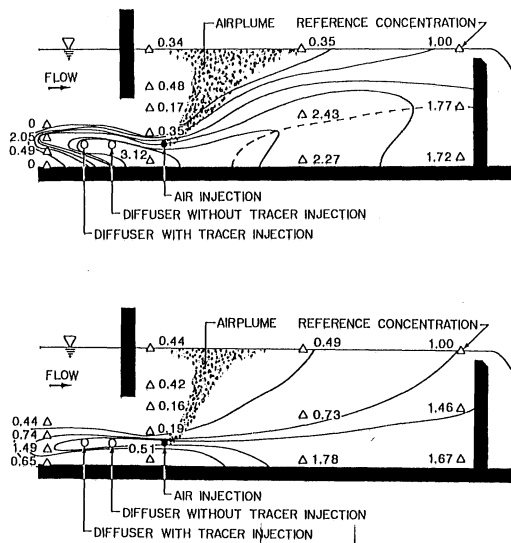


Fig. 4. Mean dye concentrations measured in the field (top) and mean conductivity distribution measured in model experiments (bottom). The means are relative to the value of the overflow.

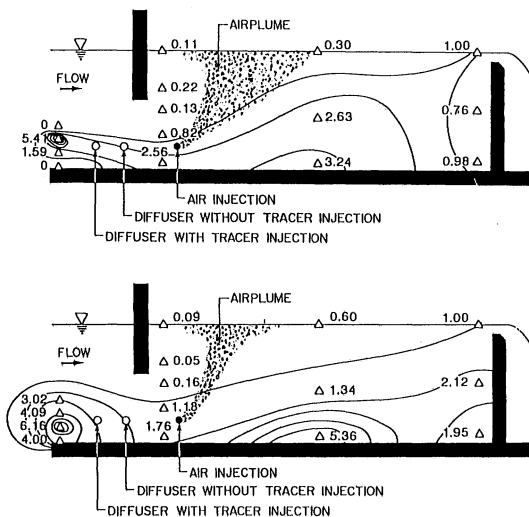


Fig. 5. Standard deviations of dye concentration in the field (top) and standard deviations of conductivity in the model (bottom). Standard deviations are relative to the standard deviation at the overflow.

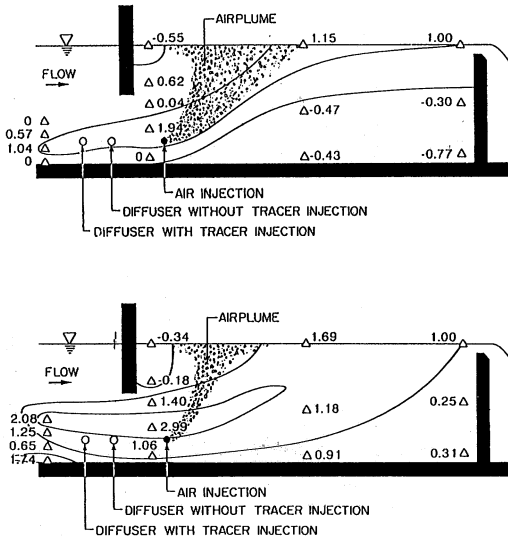


Fig. 6. Skewness of dye concentration in the field (top) and skewness of conductivity in the model (bottom). The skewness values are relative to the value of skewness at the end weir.

Methods of sampling may explain the difference. The model data was collected in-situ with a small probe capable of measuring small-scale fluctuations. The sampling in the field was conducted by continuously pumping effluent from the given locations to the fluorometer. Mixing in the pump and in the pipe en route to the fluorometer could eliminate small fluctuations in concentration. No frequency seems to be dominant in either the laboratory or the field data.

Case 2 – After Installation of Modified Diffuser and Column Wall in Basin – To increase mixing, it was recommended that a wall of 0.3 m x 0.3 m square columns be placed 1.6 m downstream of the baffle wall and that a modified SO₂ diffuser be installed (Stefan and Johnson, 1986). A diagram of the modified SO₂ diffuser is shown in Fig. 8. The new SO₂ injection system distributed the SO₂ more evenly over the inflow port. The column wall was designed to redistribute the flow uniformly over depth, break up large-scale turbulent structures and create small scale turbulence. Figure 9 shows concentration time series at the weir before and after the structural modifications.

Concentration time series were measured in both the model and field as part of a study to determine the most representative sampling point (Stefan and Johnson, 1987). Navy blue dye was used in the model as a tracer. The concentration of dye in the model basin was measured with a Konek turbidity meter connected through an A/D converter to an Apple computer. Dye concentrations were measured at steady state and were sampled at a rate of 10 samples per second for 4 minutes. Using Froude similarity, this corresponds to about 3 samples per second for 14 minutes in the prototype.

MODEL PROTOTYPE CORRELATION

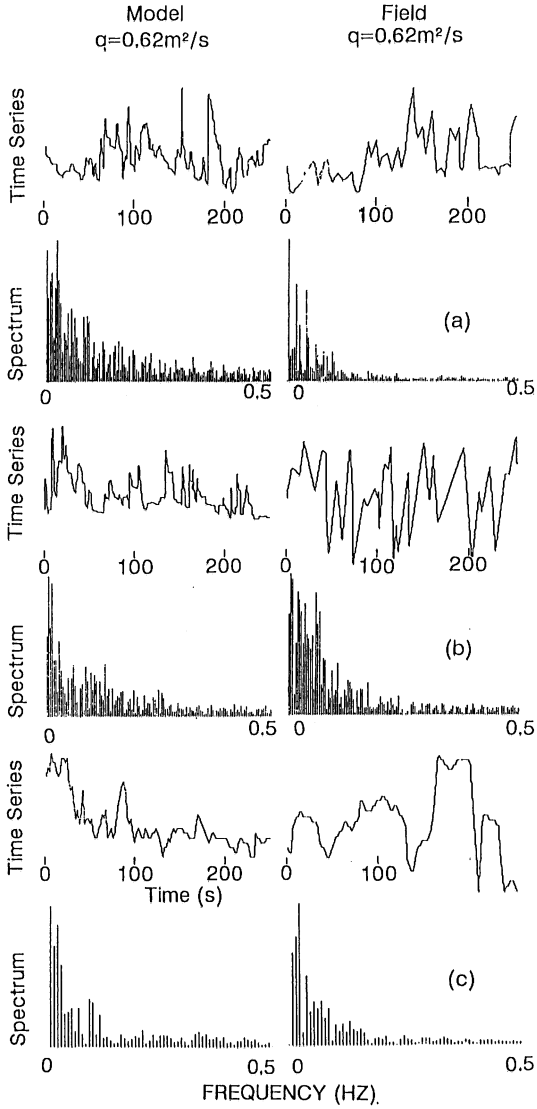


Fig. 7. Concentration time series and frequency spectra for laboratory and field data at a) .1 m below water surface and .3 m upstream from weir, b) at mid-depth in mid-basin, and c) 0.1 m below and 0.3 m downstream from edge of inlet port.

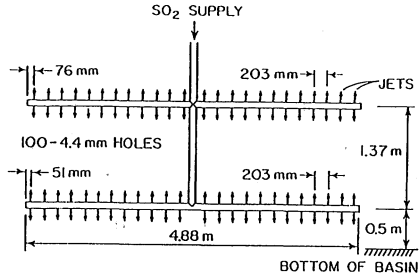


Fig. 8. Modified SO_2 diffuser (1/3 width).

The tracer and tracer injection method used in the field study was similar to that described in Case 1, but the method of data storage was different. The concentration was measured with the fluorometer once per second. Five of these one second samples were averaged to determine a five second mean. These five second means compose the field concentration time series and were recorded using a data recorder. The field data was taken at various points across the weir. Two of the locations were comparable to the locations where data was obtained in the model study.

In order to provide a direct comparison between the model and prototype, the model data was put in a form similar to the field data.

The flow rate in the field was between two flow rates which had been studied in the model. Table 1 gives the results of the model and field data analysis. Mean concentrations were normalized with cross-sectional averages. Mean values of field and laboratory data compare reasonably. Normalized standard deviations are of the same order of magnitude for the field and model measurements. The skewness data are inconclusive. A spectral analysis yielded no dominant frequencies which could be related to the vortex shedding behind the column wall.

Considerations of Turbulence Mechanisms and Scales

The concentration records analyzed here measure the degree of mixing (uniformity of concentrations) achieved in the flow. They are only indirect measures of turbulence. Direct turbulence measurements were not made. Transport and mixing of a tracer are related to advective, turbulent velocities by the transport equation

$$\frac{\partial(uC)}{\partial x} + \frac{\partial(vC)}{\partial y} + \frac{\partial(wC)}{\partial z} = -\frac{\partial C}{\partial t}$$

where the velocity component and concentrations can be thought of as composed of time-averages and fluctuating components. The fluctuating terms can be lumped into turbulent diffusion terms of the form $-D(\partial C/\partial x) = u'C'$ where D = turbulent diffusion coefficient, u' = fluctuating component of velocity, and C' = fluctuating component of concentration. The turbulent diffusion coefficient D is proportional to a turbulence length scale ℓ and a shear velocity u_* which is a measure of local shearing action. Turbulence scales and shear distributions therefore are related to turbulent mixing.

Table 1. Statistical Parameters of Dye Concentration Time Series After Structural Modifications in Basin.

Location	Elev. above bottom	Q (m^2/s)	\bar{X}/\bar{X}_{AVE}	S/\bar{X}	C_s/\bar{X}
Point A model	2.3	.27	102	0.057	0.219
Point A model	2.5	.47	109	0.047	-0.119
Point A field	2.3	.35	102	0.038	0.013
Point B model	1.2	.27	99	0.020	-0.03
Point B model	1.2	.47	99	0.030	0.552
Point B1 field	1.2	.35	114	0.081	-0.002
Point B1 field	1.2	.35	100	0.033	0

Point A is 0.1 m below water surface, 0.3 m upstream from weir. Points B1 and B2 are 1.2 m from bottom, 0.3 m upstream from weir. B1 and B2 are separated 6 m horizontally.

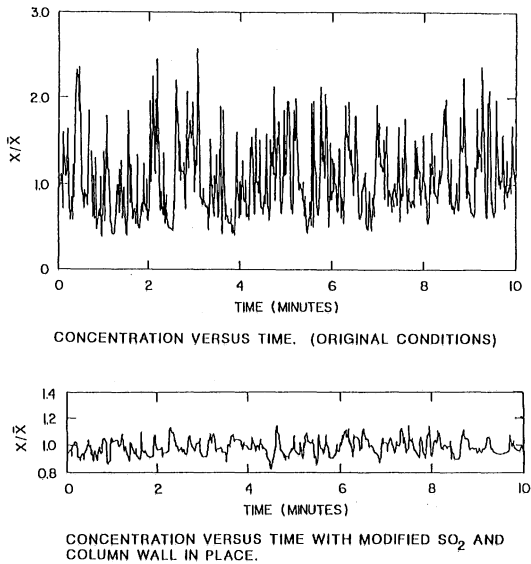


Fig. 9. Concentration time series before (Case 1) and after (Case 2) modification of the model dechlorination basin. Measurements were taken 0.3 m upstream from the weir and 0.3 m below the weir crest.

While the turbulent diffusion coefficients can be interpreted as the local rate coefficients of mixing, the measurement of concentrations at a location gives the cumulative effect of mixing, integrated along a pathline and over a travel time. The measured concentrations therefore do not indicate a local behavior.

In the flow field investigated here are several regions with very different turbulence characteristics. The main source of turbulence which produces the mixing in the basin is thought to be the shear layer between the jet-like inflow through the ports and the ambient water (a large, separated flow region exists above the inlet, see Fig. 3). Wall shear on the basin floor and the airplume contribute as well. Much of the turbulence in the upstream approach flow channel is probably dampened by the straining of eddies passing through the inlet ports. The SO_2 and air manifold pipes contribute to small scale turbulence as do the SO_2 or tracer jets discharged from them. When the column wall is added, an additional dimension of turbulence is added by the column size.

The length and velocity scales of these different regions range from very small to very large and are summarized in Table 2. Reynolds numbers were calculated for a water temperature of 20° (68°F). They are all in the turbulent range, except for the smallest scales (tracer jets and manifolds) which do not carry much significance for turbulence because of the small momentum input from tracer relative to the water flow (Table 3). Jet mixing has, however, significance for the initial dilution of the injected tracer and is a Reynolds number dependent process (Kuhlman, 1985).

The air injected downstream from the baffle wall also affects the mixing shape in the basin. The bubble size and therefore the rise velocity and path were not similar and may account for some of the differences between the model and prototype. Air bubbles in the model were too large.

Some three dimensional effects may not have been present in the model that were present in the prototype, since only a section of the basin was modeled. The prototype basin contained 6 inflow ports and 9 weir openings. (Fig. 1.) The necessary horizontal flow expansion creates large separated flow regions near the sidewalls of the basin. The effect of this expansion on the basin mixing was not modeled in the sectional model.

Conclusions

The experimental investigation of mixing in a physical scale model of complex geometry can give representative results even if full Reynolds similarity is not possible. This is illustrated for a case study of a wastewater dechlorination basin studied at a geometrical scale ratio of 1:12 using Froude similarity. Basin inflow Reynolds numbers were scaled 1:42 and were from 11,000 to 42,000 in the model based on inflow port characteristics.

Mean tracer concentrations, standard deviations and skewness of concentration fluctuations were of comparable magnitudes in model and prototype.

Nevertheless, there were subtle secondary differences of flow and mixing patterns between model and prototype. All of them can be related to the difference in Reynolds numbers. These include:

Table 2. Reynolds Numbers (final design)

		Prototype	Model
Tracer jets			
Diameter	D_o (m)	.0044	.00037
	V_o (m/s)	3.45	1.00
	Re	15,000	370
Manifold			
Diameter	D (m)	.076	.006
	V (m/s)	.35-1.31	.1-.37
	Re	27,000-99,000	600-2200
Port inlet to basin			
Depth	h (m)	.37	1.14
	V (m/s)	.35-1.31	.1-.37
	Re	480,000-1,800,000	1,000-42,000
Approach channel			
Depth	h (m)	2.7-3.7	.23-.31
	V (m/s)	.073-.35	.021-.10
	Re	270,000-960,000	6500-23,000
Column wall			
Width	d (m)	.3	.025
	V (m/s)	.15-.70	.042-.20
	Re	45,000-210,000	1,100-5,000

Table 3. Momentum Flows

	Prototype	Model
Tracer Jets (N/jet)	.18	.0001
Air from manifold (N/hole)		.00006
Water through inlet port (N/port)	440-6200	.25-3.4
Water through column wall (N/space)	25-390	.014-.23

(a) Plume trajectory rose slightly more rapidly in the prototype because of earlier separation from the basin bottom.

(b) Plume width increased more rapidly in the field.

(c) Standard deviations of concentration fluctuations were larger in the model, indicating less mixing.

(d) Skewness of concentration fluctuations was larger in the model, indicating less mixing.

The installation of a modified diffuser and a column wall changed the mixing very significantly. The mixing improved because of the introduction of the separated flow through the column wall.

Appendix I – References

- Kuhlman, J. M. (1985). "Survey of nearfield Reynolds number effects and initial condition effects and nonbuoyant jets," *Proceedings, International Symposium on Modeling Environmental Flows*, Albuquerque, NM.
- McConnell, H. L. (1986). "Engineering Report on the Dechlorination Facilities at MWTP, June – October, 1986," Metropolitan Waste Control Commission, St. Paul, MN, Engineering Construction Dept., December.
- Stanley, W. D. and Peterson, S. J. (1978). Fast fourier transforms on your home computer," *Byte*, December, 14–25.
- Stefan, H. G. and Johnson, T. R. (1986). "Dechlorination basin hydraulics," *Project Report No. 250*, St. Anthony Falls Hydraulic Laboratory, University of Minnesota, Minneapolis, MN.
- Stefan, H. G. and Johnson, T. R. (1987). "Effluent sampling location and duration study for the Metropolitan Wastewater Treatment Plant, St. Paul, Minnesota," *Project Report No. 259*, St. Anthony Falls Hydraulic Laboratory, University of Minnesota, Minneapolis, MN.

Appendix II – Symbols and Definitions

$$\bar{X} = \frac{1}{n} \sum_{i=1}^n X_i = \text{mean (local)}$$

$$S = \left[\sum_{i=1}^n \frac{(X_i - \bar{X})^2}{(n-1)} \right]^{1/2} = \text{standard deviation}$$

$$C_s = n \sum_{i=1}^n \frac{(X_i - \bar{X})^3}{(n-1)(n-2)S^3} = \text{skewness coefficient}$$

X_i = discrete sample value of concentration at a given location and time

\bar{X}_{ave} = cross sectional and temporal average of concentration
(representative of fully mixed conditions).

n = number of samples

$$\text{Re} = \frac{U_p h}{\nu} = \text{Reynolds number}$$

U_p = mean flow velocity through port

h_p = port height

ν = kinematic viscosity

$$\text{Fr} = \frac{U_p}{\sqrt{gh_p}} = \text{Froude number}$$

g = acceleration of gravity